3D flow of Carreau polymer fluid over variable thickness sheet in a suspension of microorganisms with Cattaneo-Christov heat flux

P. Durga Prasad[a], S.V. K. Varma[a], C.S.K. Raju[2], S.A. Shehzad[c,*] and M.A. Meraj[c]
[a]*Department of Mathematics,*
Sri Venkateswara University, Tirupathi, 517502-A.P, India.
[b]*Department of Mathematics, GITAM University,*
Bangalore, 562163-Karnataka, India
[c]*Department of Mathematics, COMSATS University Islamabad,*
Sahiwal 57000, Pakistan,
[*]*e-mail: ali_qau70@yahoo.com*

Received 4 January 2018; accepted 10 April 2018

Numerical study of three dimensional Carreau liquid flow with heat and mass transport features over a variable thickness sheet filled with microorganisms is analyzed. We considered the non-uniform heat sink or source and multiple slip effects. The governing non-linear partially differential expressions are developed into ordinary differential systems by using variable transformations. These expressions are solved numerically by using Runge-Kutta fourth order method connected with shooting methodology. A Parametric study is implemented to demonstrate the effects of Hartmann number, Prandtl number, Weissenberg number, Peclet number, chemical reaction and heat sink/source parameters on liquid velocity, temperature and, concentration profiles. The quantities of physical interest are described within the boundary layer. From this analysis, we found that the magnetic parameter decrease the local Sherwood and local Nusselt numbers for both $n = 1$ and $n = 0.5$ cases. The constraint of chemical reaction enhances the mass transfer rate and decelerates the density of motile mass transfer rate. The space dependent and temperature dependent heat source/sink suppress the local Nusselt number.

Keywords: Microorganisms; multiple slips; Carreau fluid; Cattaneo-Christov heat flux; 3D and slendering sheet.

PACS: 47.10.A-; 47.15.Cb

1. Introduction

The characterization of non-Newtonian fluids plays an important role in the fields of Science and Engineering. Especially for the Chemical Engineering industry the most important property of fluids is the non-Newtonian viscosity. The generalized Newtonian fluids are those in which the viscosity of the fluid depends on the shear rate. The change in the viscosity by two or three orders of magnitude is feasible for some fluids, and this cannot be ignored when the lubrication problems and polymer processing is considered. Therefore, one of the basic empirically obtained modifications of the Newton's law of viscosity is to allow the viscosity to change with the shear rate. Such variety of fluids is commonly referred to as generalized Newtonian fluids and explained by Bird [1]. The simplest generalized Newtonian fluid is the power-law constitutive relation. The power-law viscosity model has the limitation that it cannot adequately predict the viscosity for very small or very large shear rates. In view of such limitation of the power law model, generally for very large and very small shear rates, we use another viscosity model from the class of generalized Newtonian fluids, namely Carreau rheological model. This model overcomes the limitations of the power-law model identified above, and appears to be gaining wider acceptance in Chemical Engineering and technological processes. The rheology of various polymeric solutions can be explored by the Carreau liquid. In view of this, Akbar and Nadeem [2] analyzed the blood as Carreau fluid in tapered artery. Khan *et al*. [3] applied the Runge-Kutta Fehlberg method to solve momentum and temperature equations assuming MHD stagnant Carreau fluid over moving surface with convective boundary condition. Khan *et al*. [4] investigated the heat transfer characteristics of squeezed Carreau fluid flow over a sensor surface in the presence of variable thermal conductivity. The stretching phenomenon of Carreau polymer liquid with Robin's conditions has been identified by Hayat *et al*. [5].

At present, the phenomenon of heat transport has vital importance in several branches of technology, engineering and science like nuclear reactor cooling, microelectronics etc. The applications of such phenomenon in bio-medical applications include: heat conduction in tissues, magnetic drug targeting and many others. The Fourier heat conduction law explores the heat transfer mechanism since two centuries in appropriate situations. The main drawback of this law is that any disturbance created at the initial state affects the whole system. To overcome this drawback, Cattaneo [6] modified Fourier law and obtained hyperbolic energy equation by incorporating thermal relaxation time. This is later developed by Christov [7] to obtain material invariant formulation by adopting Oldroyd's derivatives. Hayat *et al*. [8] analyzed the Impact of Cattaneo-Christov heat flux model in flow of variable thermal conductivity fluid over a variable thicked surface. Li *et al*. [9] examined the features of Cattaneo-Christov model of heat diffusion in vertical stretched flow of non-Newtonian liquid. Flow between two rotating disks in

the presence of theory of Cattaneo-Christov for heat diffusion has been discussed by Hayat *et al*. [10]. The fractional model of Cattaneo-Christov heat diffusion formula is developed by Liu *et al.* [11]. Abbasi *et al*. [12] considered the two-type non-Newtonian liquids to describe the behavior of Cattaneo-Christov heat flux formula. Darcy-Forchheimer porosity flow of Jeffrey liquid with non-uniform conductivity and theory of Cattaneo-Christov for heat flux has been elaborated by Meraj *et al*. [13].

Magnetic fields are copiously used in various manufacturing industries include MHD power generators, flow meters, pumps, in the design of cooling system, purification of molten metal's from metallic inclusions with liquid metals, etc. Recently the analysis of MHD flow and heat transfer gained significance due to its applications. For example, several metallurgical processes involve cooling of continuous filaments or strips. During this process these strips are stretched through a fluid, the quality of the end product depends on the rate of cooling, and the rate of cooling of these final products with desired quality is accomplished by using electrically conducting fluids with applications of magnetic fields. The electrically conducting flow with microorganisms has much more importance in various processes of industry and engineering. According to such strong importance of this phenomenon, Mehryan *et al*. [14] inserted the motile gyrotactic micro-organisms and nanoparticles to discuss the heat transport in viscous liquid flow. Devi and Prakash [15] elaborated the results of non-uniform viscosity and conductivity flow of MHD viscous liquid induced by slendering surface. Sekhar *et al*. [16] imposed different slip condition on flow of MHD liquid flow. Palani and Kim [17] described the nature of thermal radiation in convective viscous liquid flow generated by the rotation of cone. Kuznetsov [18] demonstrated a boundary layer flow of bio convection suspension of gyrotactic-microorganisms with finite depth heated from below. Many authors analyzed MHD with different flow characterizes have been modulated by [19-27]. Zhang and Zheng [28] demonstrated that the analysis of magnetohydrodynamic thermos-solutal convection with the heat generation and first order chemical reaction can be computed by double-parameter transformation perturbation expansion method and Pade's approximant technique. They found the wall velocity is non-zero due to the Marangoni or surface tension effect which causes to decrease with increase in magnetic field parameter. The magnetohydrodynamic flow and radiation heat transfer of nanofluids in porous media with variable surface heat flux in the presence of chemical reaction was studied by Zheng *et al*. [29]. They observed that the solutal boundary layer thickness increased by increase in chemical reaction parameter.

To author knowledge, there exists no such analysis that simultaneously described the impacts of chemical reaction and heat sink/source on the fluid flow suspending microorganisms. The further novelty of this work is the utilization of Cattaneo-Christov model of heat diffusion. In this paper the steady laminar mixed convection three dimensional heat and mass transfer flow of electrically conducting Carreau fluid over a stretching sheet in a suspension of microorganisms in the presence of multiple slips. The influences of the Weissenberg number, thermal relaxation parameter, magnetic parameter, Prandtl number, heat generation/absorption parameter, Peclet number, Lewis number, and chemical reaction parameter on various quantities are discussed.

2. Mathematical Formulation

In the present investigation, we considered the Cattaneo-Christov heat flux on MHD three-dimensional flow over a variable thickness sheet. To emerge the temperature and concentration fields, gyro-tactic microorganisms and non-uniform heat source or sink are considered. The x-axis is considered along the sheet motion and y-axis is perpendicular to it as depicted in Fig. 1. Assuming $Z = A(x+y+b)^{(1-m)/2}$, $u_w(x) = U_0(x+y+c)^m$, $v_w = 0$, $m \neq 1$ and external electric field is negligible.

With these suppositions, the governing equations of continuity, momentum, thermal and mass species equations are [8]:

$$\frac{\partial u}{\partial x} + \frac{\partial v}{\partial y} + \frac{\partial w}{\partial z} = 0, \tag{1}$$

$$\left(\frac{u\partial u}{\partial x} + \frac{v\partial u}{\partial y} + \frac{w\partial u}{\partial z}\right) = \frac{\mu}{\rho}\frac{\partial^2 u}{\partial z^2}\left[1+\Gamma^2\left(\frac{\partial u}{\partial z}\right)^2\right]^{(n-1)/2} + \frac{\mu}{\rho}(n-1)\Gamma^2\frac{\partial^2 u}{\partial z^2}\left(\frac{\partial u}{\partial z}\right)^2\left[1+\Gamma^2\left(\frac{\partial u}{\partial z}\right)^2\right]^{(n-3)/2} - \sigma B^2 u, \tag{2}$$

$$\left(\frac{u\partial v}{\partial x} + \frac{v\partial v}{\partial y} + \frac{w\partial v}{\partial z}\right) = \upsilon\frac{\partial^2 v}{\partial z^2} - \sigma B^2 v, \tag{3}$$

$$\left(\frac{u\partial T}{\partial x} + \frac{v\partial T}{\partial y} + \frac{w\partial T}{\partial z}\right) + \lambda\left(\left(u\frac{\partial u}{\partial x} + v\frac{\partial u}{\partial y} + w\frac{\partial u}{\partial z}\right)\frac{\partial T}{\partial x}\right) + \left(u\frac{\partial v}{\partial x} + v\frac{\partial v}{\partial y} + w\frac{\partial v}{\partial z}\right)\frac{\partial T}{\partial y} + \left(u\frac{\partial w}{\partial x} + v\frac{\partial w}{\partial y} + w\frac{\partial w}{\partial z}\right)\frac{\partial T}{\partial z} + u\frac{\partial v}{\partial x}\frac{\partial T}{\partial y} + v\frac{\partial u}{\partial y}\frac{\partial T}{\partial x} + 2uv\frac{\partial^2 T}{\partial x\partial y} + 2vw\frac{\partial^2 T}{\partial y\partial z} + 2uw\frac{\partial^2 T}{\partial x\partial z} + u^2\frac{\partial^2 T}{\partial x^2} + v^2\frac{\partial^2 T}{\partial y^2} + w^2\frac{\partial^2 T}{\partial z^2}\right) = \alpha\frac{\partial^2 T}{\partial z^2} + q''', \tag{4}$$

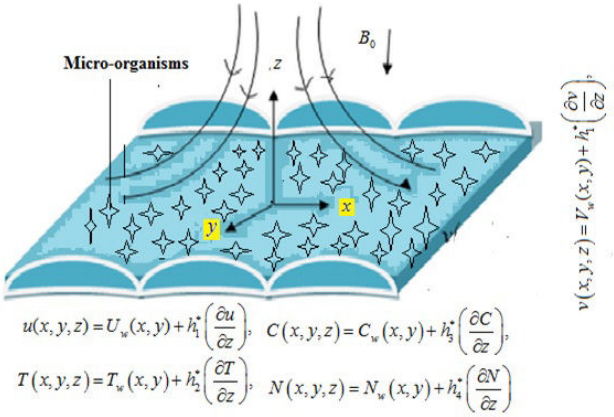

FIGURE 1. Flow configuration of the problem.

$$u\frac{\partial C}{\partial x}+v\frac{\partial C}{\partial y}+w\frac{\partial C}{\partial z}=D_m\frac{\partial^2 C}{\partial z^2}+\frac{D_T}{T_\infty}\frac{\partial^2 T}{\partial z^2}-k_0(C-C_\infty), \tag{5}$$

$$u\frac{\partial N}{\partial x}+v\frac{\partial N}{\partial y}+w\frac{\partial N}{\partial z}=D_n\frac{\partial^2 N}{\partial z^2}-\frac{bW_c}{\Delta C}\left(\frac{\partial N}{\partial z}\frac{\partial C}{\partial z}+\frac{\partial^2 C}{\partial z^2}\right), \tag{6}$$

The corresponding boundary conditions are

$$\begin{aligned}
u(x,y,z)&=U_w(x,y)+h_1^*\left(\frac{\partial u}{\partial z}\right),\\
v(x,y,z)&=V_w(x,y)+h_1^*\left(\frac{\partial v}{\partial z}\right),\\
T(x,y,z)&=T_w(x,y)+h_2^*\left(\frac{\partial T}{\partial z}\right),\\
C(x,y,z)&=C_w(x,y)+h_3^*\left(\frac{\partial C}{\partial z}\right),\\
N(x,y,z)&=N_w(x,y)+h_4^*\left(\frac{\partial N}{\partial z}\right) \quad \text{at} \quad z=0\\
u&=0, \quad v=0, \quad T=T_\infty,\\
C&=C_\infty, \quad N=N_\infty \quad \text{at} \quad z=\infty
\end{aligned} \tag{7}$$

where

$$\begin{aligned}
h_1^*&=\left[\frac{2-f_1}{f_1}\right]\xi_1(x+y+c)^{(1-n)/2},\\
\xi_2&=\left(\frac{2\gamma}{\gamma+1}\right)\frac{\xi_1}{Pr},
\end{aligned} \tag{8}$$

$$\begin{aligned}
h_2^*&=\left[\frac{2-b}{b}\right]\xi_2(x+y+c)^{(1-n)/2},\\
\xi_3&=\left(\frac{2\gamma}{\gamma+1}\right)\frac{\xi_2}{Pr},
\end{aligned} \tag{9}$$

$$\begin{aligned}
h_3^*&=\left[\frac{2-d}{d}\right]\xi_3(x+y+c)^{(1-n)/2},\\
\xi_4&=\left(\frac{2\gamma}{\gamma+1}\right)\frac{\xi_3}{Pr},\\
h_4^*&=\left[\frac{2-e}{e}\right]\xi_4(x+y+c)^{(1-n)/2},
\end{aligned} \tag{10}$$

$$B(x,y)=B_0(x+y+c)^{(1-n)/2}, \tag{11}$$

$$\begin{aligned}
U_w(x)&=a(x+y+c)^{(n-1)/2},\\
V_w(x)&=a(x+y+c)^n,\\
T_w(x)&=T_\infty+T_0(x+y+c)^{(1-n)/2},\\
C_w(x)&=C_\infty+C_0(x+y+c)^{(1-n)/2}\\
N_w(x)&=N_\infty+N_0(x+y+c)^{(1-n)/2}
\end{aligned} \tag{12}$$

The irregular heat source/sink parameter q''' is described as

$$q'''=\frac{k_f U_w(x)}{(x+y+z)\nu}(A*(T_w-T_\infty)f'+B*(T_w-T_\infty)). \tag{13}$$

From the equation above, $A*>0$, $B*>0$ represents the internal heat generation while $A*<0$, $B*<0$ denotes the heat absorption coefficients respectively. Now, as we transform the partial equations into ordinary differential equations we introduce the similarity transformation as

$$\begin{aligned}
\eta&=z\sqrt{\frac{(n+1)a}{2\upsilon}(x+y+c)^{n-1}},\\
\theta&=\frac{T-T_\infty}{T_w(x)-T_\infty},\\
\phi&=\frac{C-C_\infty}{C_w(x)-C_\infty}, \quad \chi=\frac{N-N_\infty}{N_w(x)-N_\infty}\\
u&=a(x+y+c)^n f'(\eta), \quad v=a(x+y+c)^n g'(\eta)\\
w&=\sqrt{\frac{2a\upsilon}{n+1}(x+y+c)^{n-1}}\\
&\times\left[\frac{n+1}{2}(f+g)+\eta\left(\frac{n-1}{2}\right)(f'+g')\right]
\end{aligned} \tag{14}$$

with the help of (11), (12) and (13), Eqs. (2)-(4) converted as the below differential equations:

$$\frac{n+1}{2}f'''\left[1+\left(\frac{n-1}{2}\right)Wef''^2(3+(n-3)Wef''^2)\right]+\frac{n+1}{2}(f+g)f''-nf'^2-nf'g'-Mf'=0, \tag{15}$$

$$\frac{n+1}{2}g''' + \frac{n+1}{2}(f+g)g'' - ng'^2 - nf'g' - Mg' = 0, \quad (16)$$

$$\frac{n+1}{2}\theta''' - \Pr\left[\frac{1-n}{2}(f'+g')\theta - \frac{n+1}{2}(f+g)\theta'\right] + \Pr\gamma\left(\frac{m-3}{2}(f+g)(f'+g')\theta' - \frac{m+1}{2}(f+g)^2\theta''\right) + A*f' + B*\theta = 0, \quad (17)$$

$$\frac{n+1}{2}\phi'' - Le\left[\frac{1-n}{2}(f'+g')\phi - \frac{n+1}{2}(f+g)\phi' + K_r\phi\right] = 0, \quad (18)$$

$$\frac{1}{Le}\frac{n+1}{2}\chi'' - \left[\frac{1-n}{2}(f'+g')\chi - \frac{n+1}{2}(f+g)\chi' - Pe(\phi'\chi' + \phi''(\beta_1+\chi))\right] = 0, \quad (19)$$

With the corresponding boundary conditions are

$$\begin{aligned} f(0) &= \delta\left(\frac{1-n}{n+1}\right)[1+h_1 f''(0)], \\ f'(0) &= [1+h_1 f''(0)], \\ g(0) &= \delta\left(\frac{1-n}{n+1}\right)[1+h_1 g''(0)], \\ g'(0) &= [1+h_1 g''(0)], \quad \theta(0) = [1+h_2\theta'(0)], \\ \phi(0) &= [1+h_3\phi'(0)], \quad \chi(0) = [1+h_4\chi'(0)], \\ f'(\infty) &= 0, \quad g'(\infty) = 0, \\ \theta(\infty) &= 0, \quad \chi(\infty) = 0. \end{aligned} \quad (20)$$

The dimensional parameters M, Pr, Le, Nt, Nb, Kr, h_1, h_2, γ, h_3, h_4, δ pe and β_1 are given by

$$M = \frac{\sigma B_0^2}{\rho a}, \quad \Pr = \frac{\mu C_p}{k}, \quad Le = \frac{v}{D_B},$$

$$kr = \frac{k_0}{a(x+y+c)^{n-1}}, \quad Nb = \frac{\tau D_B C_0}{k_f}, \quad Nt = \frac{\tau D_T T_0}{T_\infty k_f}$$

$$\delta = A\sqrt{\frac{(n+1)a}{2v}}, \quad Pe = \frac{bW_c}{D_n}, \quad \beta_1 = \frac{N}{N-N_\infty}$$

$$h_1 = \xi_1\left(\frac{2-f_1}{f_1}\right)\sqrt{\frac{U_0(m+1}{2v}},$$

$$\gamma = \lambda_1 U_0 (x+y+c)^{m-1},$$

$$h_2 = \xi_2\left(\frac{2-f_1}{f_1}\right)\sqrt{\frac{U_0(m+1}{2v}},$$

$$h_3 = \xi_3\left(\frac{2-f_1}{f_1}\right)\sqrt{\frac{U_0(m+1}{2v}},$$

$$h_4 = \xi_4\left(\frac{2-f_1}{f_1}\right)\sqrt{\frac{U_0(m+1}{2v}}.$$

The skin-friction coefficient C_f, local Nusselt Nu_x and Sherwood number Sh_x are defined as

$$C_f = \frac{\mu\frac{\partial u}{\partial z}}{\frac{1}{2}\rho U_w^2}, \quad Nu_x = \frac{(x+y+c)\frac{\partial T}{\partial z}}{T_w(x) - T_\infty},$$

$$Sh_x = \frac{(x+y+c)\frac{\partial N}{\partial z}}{N_w(x) - N_\infty}, \quad (21)$$

$$\begin{aligned} C_f(Re_x)^{0.5} &= 2\sqrt{\frac{m+1}{2}}\left(1 + \left(\frac{n-1}{2}\right)\right. \\ &\quad \left.\times We f''^2(3 + (n-3)We f''^2)\right) f''(0), \\ Nu_x(Re_x)^{-0.5} &= -\sqrt{\frac{m+1}{2}} \\ &\quad \times \left(\Pr\gamma\frac{m+1}{2}(f+g)^2 + 1\right)\theta'(0) \\ Sh_x(Re_x)^{-0.5} &= -\sqrt{\frac{m+1}{2}}\phi'(0), \\ Sh_x(Re_x)^{-0.5} &= -\sqrt{\frac{m+1}{2}}\chi'(0) \end{aligned} \quad (22)$$

Where $Re_x = U_x X/v$ and $X = (x+b)$

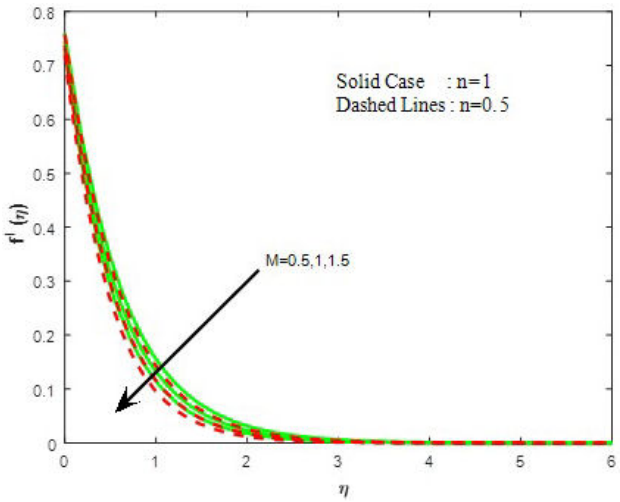

FIGURE 2. Impact of M on $f'(\eta)$.

TABLE I. Values of local friction factor for different physical governing parameters for $n = 1$ and $n = 0.5$ cases.

M	We	Kr	γ	Pe	A^*	B^*	β_1	$-f''(0)$		$-g''(0)$	
								$n=1$	$n=0.5$	$n=1$	$n=0.5$
0.5								1.198579	1.204921	1.213151	1.219822
1.0								1.276179	1.284636	1.314271	1.323920
1.5								1.345101	1.355883	1.400997	1.413920
	1							1.108638	1.210664	1.119063	1.224781
	3							0.915229	1.226421	0.921319	1.238011
	5							0.808500	1.236994	0.813276	1.246745
		0.1						1.198579	1.204921	1.213151	1.219822
		0.3						1.198579	1.204921	1.213151	1.219822
		0.5						1.198579	1.204921	1.213151	1.219822
			0.1					1.198583	1.204917	1.213148	1.219819
			0.3					1.198579	1.204921	1.213152	1.219822
			0.5					1.198579	1.204921	1.213152	1.219822
				0.1				1.198585	1.204921	1.213151	1.219822
				0.4				1.198579	1.204921	1.213151	1.219822
				0.7				1.198573	1.204921	1.213151	1.219822
					0.1			1.198579	1.204921	1.213150	1.219821
					0.4			1.198578	1.204921	1.213150	1.219821
					0.7			1.198578	1.204921	1.213144	1.219820
						0.1		1.198579	1.204921	1.213150	1.219821
						0.15		1.198579	1.204921	1.213151	1.219822
						0.2		1.198579	1.204921	1.213152	1.219822
							0.1	1.198579	1.204921	1.213151	1.219822
							0.3	1.198579	1.204921	1.213151	1.219822
							0.5	1.198579	1.204921	1.213151	1.219822

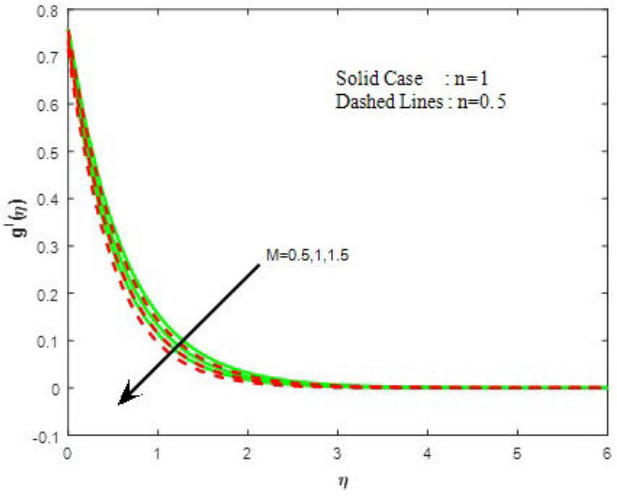

FIGURE 3. Impact of M on $g'(\eta)$.

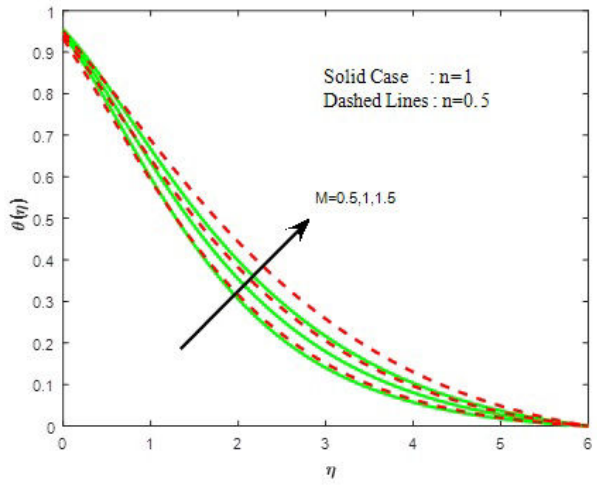

FIGURE 4. Impact of M on $\theta(\eta)$.

3. Results and Discussion

The set of ordinary differential Eqs. (15)-(19) are solved numerically by applying Runge-Kutta fourth order method with shooting technique. The numerical values of non-dimensional parameters such as M, We, k_r, γ, Pe, $A*$, $B*$, β_1, and β_1, on local skin friction coefficient, local Nusselt number and Sherwood numbers are demonstrated in the Tables I and II. In the present investigation, we examine two cases such as Newtonian and non-Newtonian, and obtained dual solutions

TABLE II. Values of local Nusselt, Sherwood number and motile Sherwood numbers for different physical governing parameters for $n = 1$ and $n = 0.5$ cases.

M	We	Kr	γ	Pe	A^*	B^*	β_1	(Nu_x)		Sh_x		MSh_x	
								$n = 1$	$n = 0.5$	$n = 1$	$n = 0.5$	$n = 1$	$n = 0.5$
0.5								0.280175	0.333139	0.582159	0.670933	0.128627	0.197692
1.0								0.249072	0.289382	0.569954	0.650575	0.112324	0.171775
1.5								0.221223	0.248416	0.559690	0.633886	0.099315	0.151585
	1							0.285105	0.339112	0.585471	0.675937	0.131859	0.202557
	3							0.300297	0.355684	0.595672	0.690700	0.143005	0.218644
	5							0.311365	0.366383	0.603558	0.701693	0.152836	0.232245
		0.1						0.280175	0.333139	0.509237	0.606086	0.163399	0.227578
		0.3						0.280175	0.333139	0.642994	0.725634	0.100818	0.173453
		0.5						0.280175	0.333139	0.742534	0.816177	0.057197	0.134867
			0.1					0.263228	0.336052	0.582158	0.670931	0.128630	0.197698
			0.3					0.270681	0.334158	0.582159	0.670933	0.128627	0.197692
			0.5					0.280175	0.333139	0.582159	0.670933	0.128627	0.197692
				0.1				0.280176	0.333139	0.582158	0.670933	0.357354	0.458658
				0.4				0.280175	0.333139	0.582159	0.670933	0.184660	0.262361
				0.7				0.280175	0.333139	0.582159	0.670933	0.019269	0.069907
					0.1			0.323435	0.385548	0.582159	0.128627	0.670933	0.197692
					0.4			0.193656	0.228322	0.582159	0.128627	0.670933	0.197692
					0.7			0.063877	0.071093	0.582159	0.128627	0.670933	0.197692
						0.1		0.280175	0.333139	0.582159	0.670933	0.128627	0.197692
						0.15		0.197842	0.218259	0.582159	0.670933	0.128627	0.197692
						0.2		0.083141	0.009758	0.582159	0.670933	0.128627	0.197692
							0.1	0.280175	0.333139	0.582159	0.670933	0.174098	0.258137
							0.3	0.280175	0.333139	0.582159	0.670933	0.151362	0.227915
							0.5	0.280175	0.333139	0.582159	0.670933	0.128627	0.197692

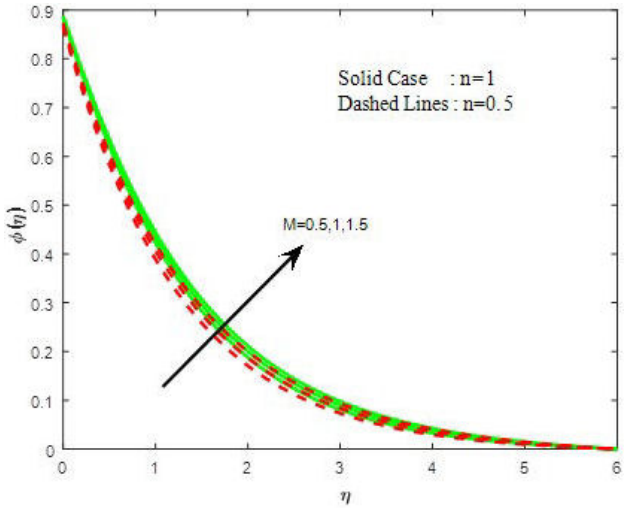

FIGURE 5. Impact of M on $\phi(\eta)$.

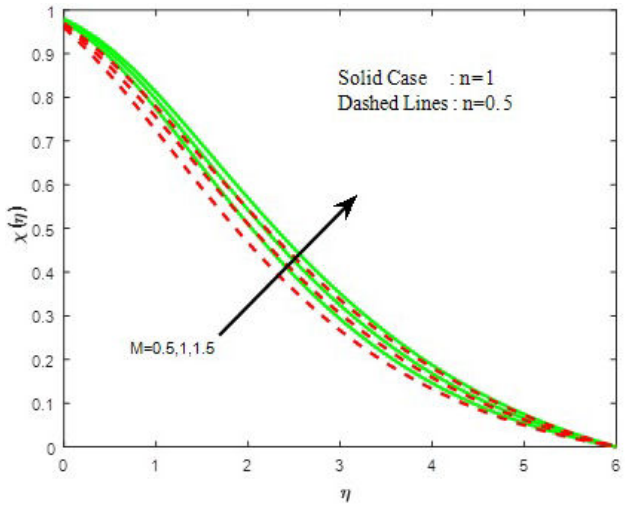

FIGURE 6. Impact of M on $\phi(\eta)$.

by keeping $n = 0.5$ and $n = 1$ for Newtonian and non-Newtonian fluids.

Figures 2-6 show the effect of the magnetic parameter on velocities, temperature, concentration and density of motile organism for both Newtonian ($n = 1$) and non-Newtonian ($n = 0.5$) liquids. From Figs. 2 and 3, it is evident that the strength of magnetic field is to diminish the velocities. This reduction can be attributed to the fact that the magnetic field provides a resisting type force known as the Lorentz force.

This force tends to lessen the motion of liquid and as a consequence, the velocity depreciates. From Fig. 4, temperature is found to be enhancing with the magnetic field. Here the frictional resistance on account of the magnetic field resulting in the reduction of velocity, and there by, enhances the temperature. The effect of magnetic field performs an increasing effect on concentration and density of motile organism (see Figs. 5 and 6).

Figures 7 and 8 are plotted to demonstrate the influence of the Weissenberg number (We) on the velocities. Figure 7 investigates that the primary velocity increases with the increasing values of Weissenberg number, whereas the secondary velocity shows the opposite behavior (see Fig. 8). In Figs. 9-11, the physical behavior of the boundary layer near to the surface can be seen by observing the temperature, concentration and density of motile organism profiles respectively for various values of Weissenberg number. The profiles of temperature (Fig. 9), concentration (Fig. 10) and density of motile organism (Fig. 11) clearly depict the decreasing phenomenon with the increasing Weissenberg number.

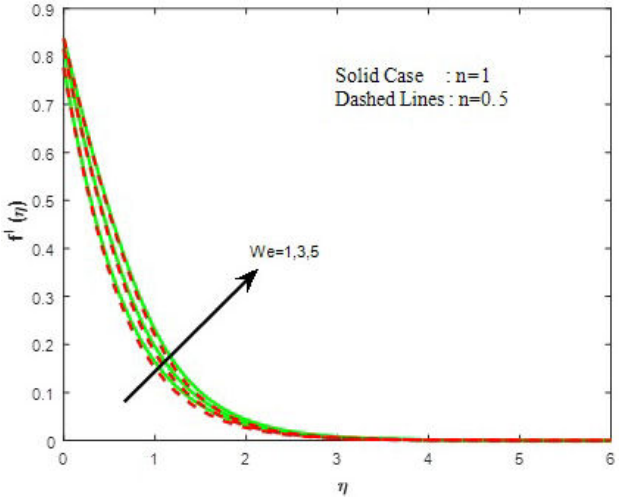

FIGURE 7. Impact of We on $f'(\eta)$.

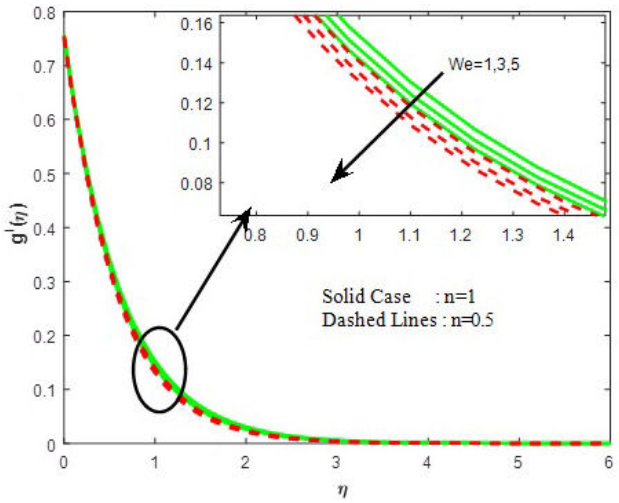

FIGURE 8. Impact of We on $g'(\eta)$.

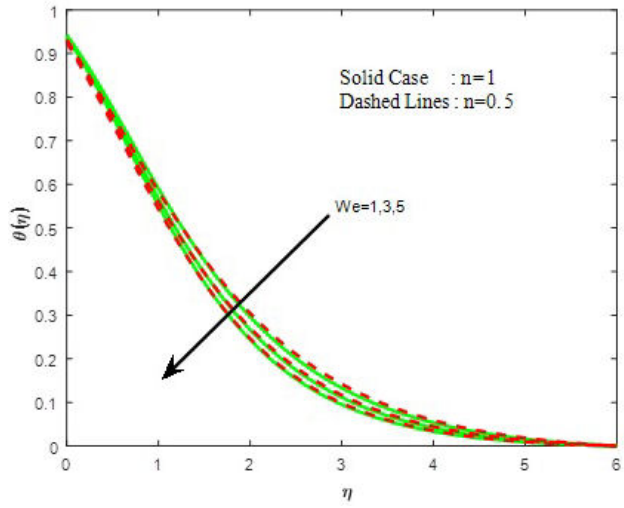

FIGURE 9. Impact of We on $\theta(\eta)$.

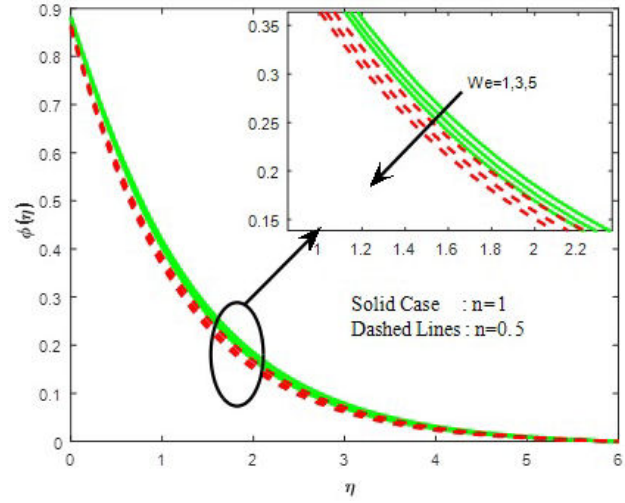

FIGURE 10. Impact of We on $\phi(\eta)$.

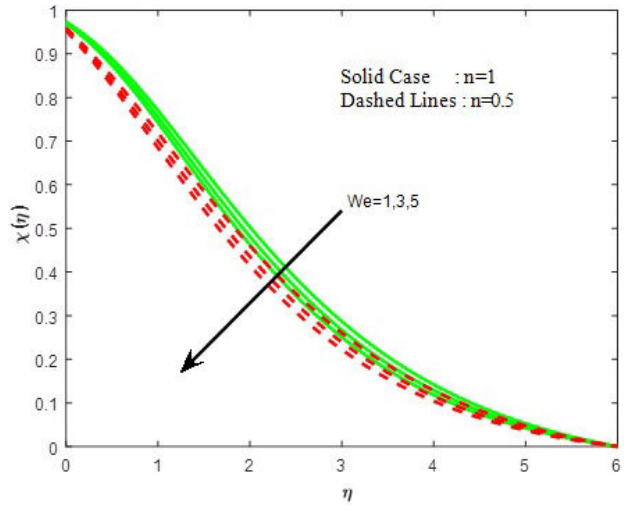

FIGURE 11. Impact of We on $\chi(\eta)$.

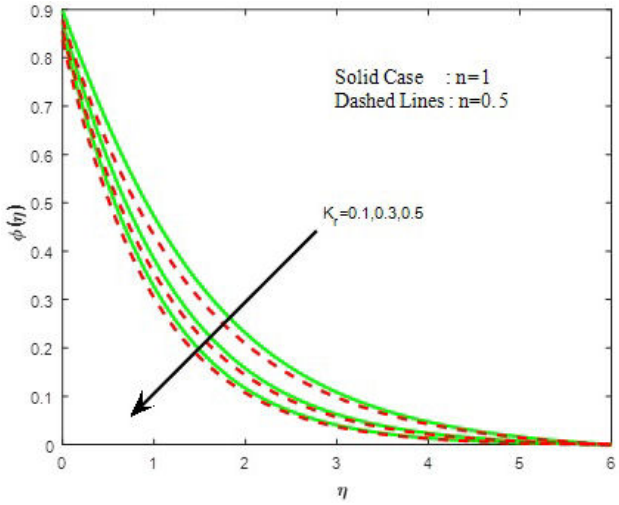

FIGURE 12. Impact of K_r on $\phi(\eta)$.

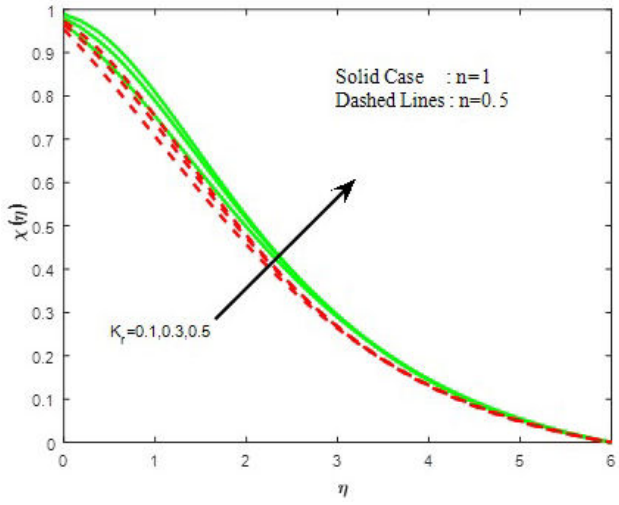

FIGURE 13. Impact of K_r on $\chi(\eta)$.

The impact of chemical reaction parameter k_r on species concentration profile is depicted in Fig. 12. It is observed that an increase in the value of chemical reaction parameter reduces the concentration of species in the boundary layer owing to the fact that destructive chemical reaction reduces the solutal boundary layer and enhances the mass transfer while it shows opposite trend on density of motile organism (see Fig. 13).

Figure 14 depicts the temperature profile for various values of thermal relaxation parameter γ. From this Fig. 14, it is evident that the temperature as well as thermal boundary layer thickness retard, with the presence of thermal relaxation parameter. This is due to the fact, that for enhancing values of thermal relaxation, time the fluid particles steadily transfer heat to its surrounding particles. Figure 15 elucidates that density of motile organism increases with increasing values of Peclet number Pe.

Figures 16 and 17 represent the plots of temperature with variation in $A*$ and $B*$. The temperature increases rapidly throughout the boundary layer due to the release of energy

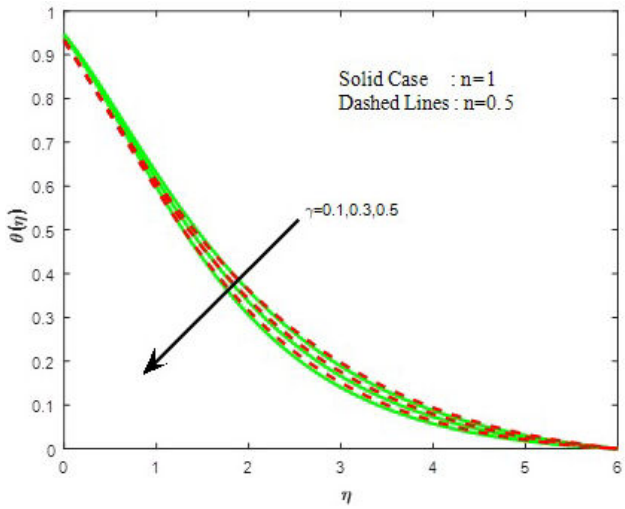

FIGURE 14. Impact of γ on $\theta(\eta)$.

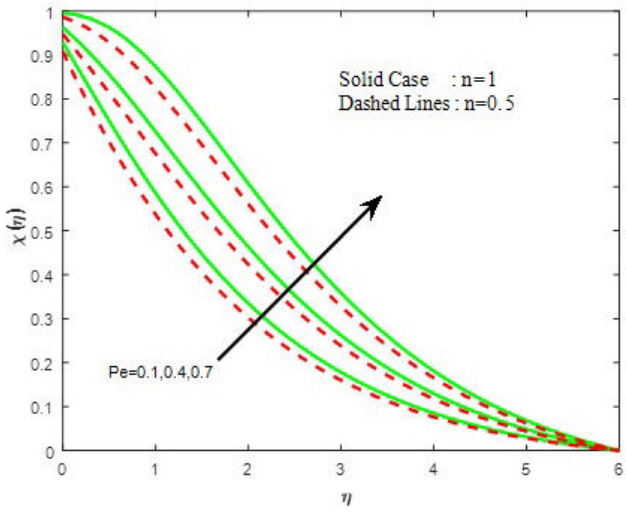

FIGURE 15. Impact of Pe on $\chi(\eta)$.

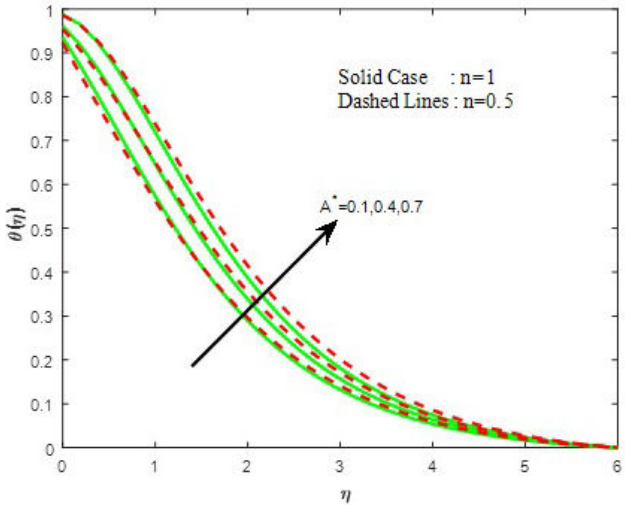

FIGURE 16. Impact of A^* on $\theta(\eta)$.

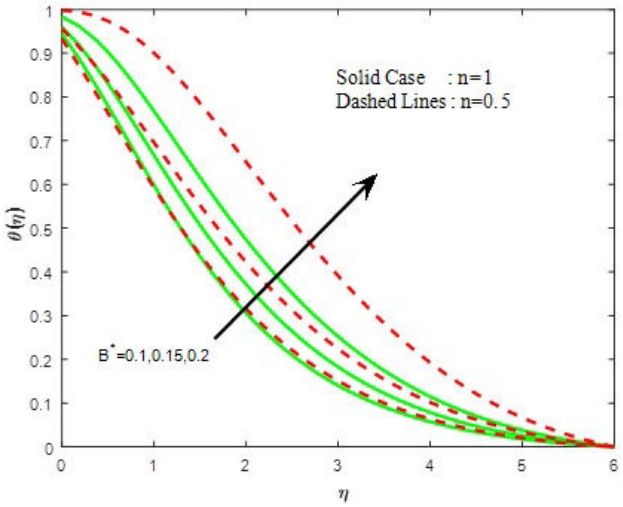

FIGURE 17. Impact of A^* on $\theta(\eta)$.

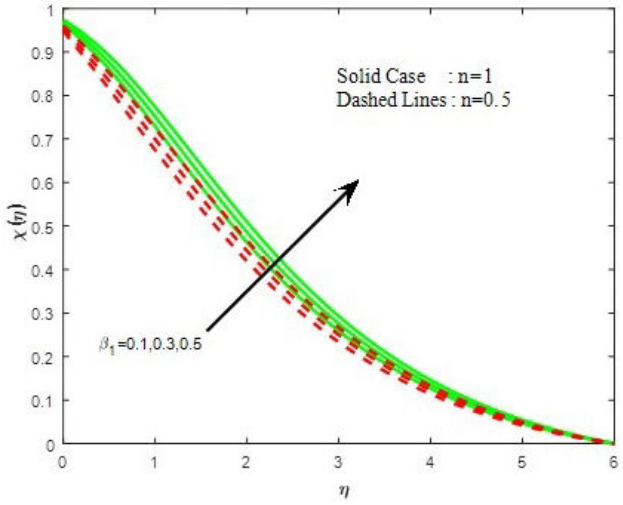

FIGURE 18. Impact of β_1 on $\chi(\eta)$.

in thermal boundary layer for increasing values of temperature dependent heat source/sink parameter. The density of motile organism increases with the increasing values of liquid parameter β_1 (see Fig. 18).

The numerical values of dimensionless friction factor for various values of physical parameters are displayed in Table I. It is observed that the skin friction coefficient increased for magnetic parameter M and thermal relaxation parameter γ for both $n = 1$ and $n = 0.5$. The local Nusselt number, local Sherwood number and motile microorganisms are studied for different physical parameters like Magnetic parameter, Weissenberg number, chemical reaction parameter, thermal relaxation parameter, Peclet number, time and space dependent parameters, and liquid parameter are investigated in Table II. From this Table, we found that the magnetic parameter decreases the local Nusselt number and local Sherwood numbers for both $n = 1$ and $n = 0.5$. An opposite phenomena can be observed for increasing values of Weissenberg number. The chemical reaction parameter enhances the mass transfer rate and decelerates the density of motile mass transfer rate. The space dependent and temperature dependent heat source/sink suppress the local Nusselt number.

4. Conclusions

The present study addresses the 3D flow of Carreau fluid over variable thickness sheet in suspension of microorganisms with Cattaneo-Christov heat diffusion formula. The key observations of this investigation can be described as:

- The temperature increases rapidly throughout the boundary layer owing to the release of energy in thermal boundary layer for increasing values of temperature dependent heat source/sink parameter.
- The profiles of temperature, concentration and density of motile organism phenomenon reduced with an increment in Weissenberg number.
- Non-Newtonian liquid showed better heat transfer performance compare with Newtonian liquid.
- The magnetic parameter decreases the local Nusselt and local Sherwood numbers for both $n = 1$ and $n = 0.5$.
- The chemical reaction parameter enhances the mass transfer rate and decelerates the density of motile mass transfer rate. The space dependent and temperature dependent heat source/sink suppress the local Nusselt number.

Compliance with ethical standards

Funding: There are no funders to report for this submission.

Conflict of Interest: The authors declare that they have no conflict of interest.

Nomenclature:

a:	Thermal accommodation coefficient
A:	Coefficient related to stretching sheet
A^*:	Dimensional stretching sheet coefficient
b:	Physical parameter related to stretching sheet
$B(xy)$:	Magnetic field with space dependent
C :	Concentration of the fluid
C_f:	Skin friction coefficient
C_p:	Specific heat capacity at constant pressure
C_s:	Concentration susceptibility
C_∞:	Concentration of the fluid in the free stream
d:	Concentration accommodation coefficient
D_m:	Molecular diffusivity of the species concentration
e:	Diffusion of organism's accommodation coefficient
f_1:	Maxwell's reflection coefficient
f, g:	Dimensionless velocities
h_1^*:	Dimensional velocity slips parameter

h_2^*: Dimensional temperature jump parameter
h_3^*: Dimensional concentration jump parameter
h_4^*: Dimensional diffusion jump
h_1: Dimensionless velocity slip parameter
h_2: Dimensionless temperature jump parameter
h_3: Dimensionless concentration jump parameter
h_4: Dimensionless diffusion jump parameter
k: Thermal conductivity
k_T: Thermal diffusion ratio
k_r: Chemical reaction parameter
Le: Lewis number
m: Velocity power index parameter
M: Magnetic field interaction parameter
n: Power-law index parameter
Nu_x: Local Nusselt number
Pr: Prandtl number
Pe: Peclet number
Re_x: Local Reynolds number
Sh_x: Local Sherwood number
MSh_x: Local motile Sherwood number
T: Temperature of the fluid
T_m: Mean fluid temperature
T_∞: Temperature of the fluid in the free stream parameter
u, v, w: Velocity components in directions
x: Direction along the surface
y: Direction normal to the surface

Greek Symbols:

β: Casson fluid parameter
β_1: Fluid parameter
η: Similarity variable
ϕ: Dimensionless concentration
χ: Density of motile organisms
σ: Electrical conductivity of the fluid
τ: Ratio of specific heats
γ: Thermal relaxation parameter
θ: Dimensionless temperature
ρ: Density of the fluid
μ: Dynamic viscosity
υ: Kinematic viscosity
δ: Wall thickness parameter
ξ_1: Mean free path (constant)

1. R.B. Bird, *The Canadian Journal of Chemical Engineering* **43** (1965) 161-168.
2. N.S. Akbar, S. Nadeem, *Ain Shams Engineering Journal* **5** (2014) 1307-1316.
3. M. Khan, Hashim, A.S. Alshomrani, *Plos One* **11** (2016) e0157180.
4. M. Khan, M.Y. Malik, T. Salahuddin, I. Khan, *Results in Physics* **6** (2016) 940-945.
5. T. Hayat, M. Waqas, S.A. Shehzad, A. Alsaedi, *Pramana* **86** (2016) 3-17.
6. C. Cattaneo, *Sullaconduzionedelcalore, in: Atti Del Seminario Matematicoe Fisico dell Universita di Modenae Reggio Emilia*, **3** (1948) 83-101.
7. C.I. Christov, *Mechanics Research Communications* **36** (2009) 481-486.
8. T. Hayat, M.I. Khan, M. Farooq, A. Alsaedi, M. Waqas, T. Yasmeen, *International Journal of Heat and Mass Transfer* **99** (2016) 702-710.
9. J. Li, L. Zheng, L. Liu, *Journal of Molecular Liquids* **221** (2016) 19-25.
10. T. Hayat, S. Qayyum, M. Imtiaz, A. Alsaedi, *Results in Physics* **7** (2017) 126-133.
11. L. Liu, L. Zheng, F. Liu, X. Zhang, *International Journal of Heat and Mass Transfer* **103** (2016) 1191-1197.
12. F.M. Abbasi, T. Hayat, S.A. Shehzad, A. Alsaedi, *International Journal of Numerical Methods for Heat & Fluid Flow* **27** (2017) 1955-1966.
13. M.A. Meraj, S.A. Shehzad, T. Hayat, F. M. Abbasi, A. Alsaedi, *Applied Mathematics and Mechanics* **38** (2017) 557-566.
14. A.M. Mehryan, F.M. Kashkooli, M. Soltani, K. Raahemifar, *Plos One* **11** (2016) e0157598.
15. S.P.A. Devi, M. Prakash, *Journal of the Nigerian Mathematical Society* **34** (2015) 318-330.
16. K. R. Sekhar, G.V. Reddy, *I-Manager's Journal on Mathematics* **6** (2017) 14-22.
17. G. Palani, K.Y. Kim, *Applied Mathematics and Mechanics* **33** (2012) 605-620.
18. A.V. Kuznetsov, *Int. Commun. Heat Mass Transfer* **32** (2005) 574-582.
19. K.R Sekhar, G.V. Reddy, S.V. K.Varma, *Elixir. Int. J.* **99** (2016) 43237-43241.
20. C.S.K. Raju, K.R. Sekhar, S.M. Ibrahim, G. Lorentzini, G.V. Reddy, E. Lorentzini, *Continuum Mechanics and Thermodynamics*, DOI 10.1007/s00161-016-0552-8.
21. C.S.K. Raju, S.M. Ibrahim, S. Anuradha and P. Priyadarsini, *The Eur. Phys. J. Plus* **131** (2016) 409.
22. K. R. Sekhar, G. Viswanatha Reddy, *J. Nanofluids* **6** (2017) 1159-1165.
23. J. Zhu, L. Zheng, L. Zheng, X. Zhang, *Applied Mathematics and Mechanics* **36** (2015) 1131-1146.
24. K. Hsiao, *Applied Thermal Engineering* **98** (2016) 850-861.
25. M. Sheikholeslami, H.B. Rokni, *International Journal of Heat and Mass Transfer* **107** (2017) 288-299.

26. M. Sheikholeslami, *Journal of Molecular Liquids* **225** (2017) 903-912.

27. M. Sheikholeslami, *Journal of Molecular Liquids* **234** (2017) 364-374.

28. Y. Zhang, L. Zheng, *Chemical Engineering Science* **69** (2012) 449-455.

29. C. Zhang, L. Zheng, X. Zhang, G. Chen, *Applied Mathematical Modelling* **39** (2015) 165-181.